

## **Short Communication**

# **Using Artificial Neural Network for Estimation of Density and Viscosities of Biodiesel–Diesel Blends**

**Gholamreza Moradi<sup>\*1</sup>, Majid Mohadesi<sup>2</sup>, Bita Karami<sup>1</sup> and Ramin Moradi<sup>3</sup>**

<sup>1</sup>Catalyst Research Center, Chemical Engineering Department, Faculty of Engineering, Razi University, Kermanshah, I. R. Iran

<sup>2</sup>Chemical Engineering Department, Faculty of Energy, Kermanshah University of Technology, Kermanshah, I. R. Iran

<sup>3</sup>Faculty of Mechanical Engineering, Sharif University of Technology, Tehran, I. R. Iran  
(Received 29 March 2015, Accepted 12 December 2015)

### **Abstract**

In recent years, biodiesel has been considered as a good alternative of diesel fuels. Density and viscosity are two important properties of these fuels. In this study, density and kinematic viscosity of biodiesel-diesel blends were estimated by using artificial neural network (ANN). A three-layer feed forward neural network with Levenberg-Marquard (LM) algorithm was used for learning empirical data (previous studies data and this study empirical data). Input data for estimating density and kinematic viscosity includes components volume fraction, temperature and pure component properties (pure density at 293.15 K and pure kinematic viscosity at 313.15 K). Results of neural network simulation for density and kinematic viscosity showed a high accuracy (mean relative error for density and kinematic viscosity are 0.021% and 0.73%, respectively).

**Keywords:** Artificial neural network, Biodiesel, Blend, Density, Kinematic viscosity.

### **1. Introduction**

Reducing energy sources and increasing cost of energy persuade humans to find new and renewable sources [1, 2]. Biodiesel is one of the most important biofuels that has been considered recently. This fuel is produced by transesterification of vegetable oils or animal fats with alcohol at presence of basic, acidic or enzymatic catalysts [3].

Biodiesel fuel has many advantages and uses. Using this fuel causes to reduce release of greenhouse gases and environment pollutant gases.

This fuel is biodegradable, non-toxic and renewable. Compared with diesel, biodiesel has higher cetane number and flash temperature. Also its combustion releases lowers amount of hydrocarbons, carbon monoxide and suspended particles. Biodiesel completely dissolves in diesel so they can combine in each percent with each other. Although biodiesel and diesel have differences, biodiesel can be used pure or blend with diesel, without any changes in diesel equipment directly [4-7].

Viscosity and density are two basic parameters of diesel engines fuels [7]. Fuels with higher viscosity need more energy for pumping [8] and also their sparing is harder, while their efficiency is lower [8, 9]. Density is the other important parameter that its increment has a positive effect on output power because fuel injection system measures fuel on the base of volume, so more mass is injected [10].

Different empirical and theoretical studies [5-9, 11-26] on density and viscosity of biodiesel-diesel blend in different temperatures has been done and many studies are presented for predicting density and viscosity. A summary of presented equations is available in Table 1. Most of presented equations have some constants that according to mixture components (biodiesel and diesel) properties can be estimated.

Artificial neural network has been used for estimating physical and chemical data in many studies recently [27-42].

**Table 1: Presented equations for predicting density and viscosity of biodiesel-diesel blend at different temperatures**

Correlation	Eq.	Source
<i>Pure correlation (temperature dependency)</i>		
$\rho = a + bT$	(1)	[5, 6, 16-18]
$\ln(\nu) = A + \frac{B}{T} + \frac{C}{T^2}$	(2)	[22]
$\ln(\nu) = A + \frac{B}{T+C}$	(3)	[23]
<i>Mixture correlation (constant temperature)</i>		
$\rho_m = v_1\rho_1 + v_2\rho_2$	(4)	[19]
$\rho_m = av_1 + b$	(5)	[19]
$\ln(\nu_m) = v_1\ln(\nu_1) + v_2\ln(\nu_2)$	(6)	[25]
$\nu_m = \left( v_1\nu_1^{1/3} + v_2\nu_2^{1/3} \right)^3$	(7)	[25]
$\nu_m = av_1^2 + bv_1 + c$	(8)	[25]
<i>Combined correlation</i>		
$\rho = \alpha V + \beta T + \delta$	(9)	[20]
$\ln(\nu) = \ln \gamma + \Phi V + \omega T + \lambda VT$	(10)	[8]
$\ln(\nu) = \ln \gamma + \Phi V + \frac{\omega}{T} + \frac{\lambda V}{T^2}$	(11)	[20]
$\ln(\nu) = \ln \gamma + \frac{\omega}{T} + \frac{\lambda V}{T}$	(12)	[20]
$\ln(\nu) = \ln \gamma + \frac{\omega}{T} + \frac{\lambda V}{T^2}$	(13)	[20]
$\ln(\nu) = \ln \gamma + \Phi V + \frac{\omega}{T} + \frac{\lambda V}{T}$	(14)	[24]
$\ln(\nu) = \ln \gamma + \Phi V + \frac{\omega}{T}$	(15)	[26]

In the current study, several biodiesels include soybean oil biodiesel (SOB), canola oil biodiesel (COB), sunflower oil biodiesel (SFOB), waste oil biodiesel (WOB) and edible tallow biodiesel (ETB) were produced and the density and kinematic viscosity of them and their blends with diesel were measured at different temperatures and volume fractions. Then, artificial neural network was used to estimate these properties. To obtain ANN models for density and kinematic viscosity, existent data in different literature [3, 16, 17 and 20] and also the measured data from our experiments were used. Density and kinematic viscosity of biodiesel-diesel blends were considered as a function of temperature, pure biodiesel and diesel properties and volume fraction of biodiesel. Consequently, it was observed that ANN

has higher accuracy compared with previous methods.

## 2. Experimental data

### 2.1. Biodiesel production

Four different vegetable oils (soybean oil, canola oil, sunflower oil and waste cooking oil) and edible tallow were used to produce biodiesel. Because of high acid numbers of waste cooking oil and edible tallow (1.23 and 9.52 mg KOH/g, respectively), a pre-esterification step was done on them to decrease acid number to less than 1 mg KOH/g. Pre-esterification was done in the presence of H<sub>2</sub>SO<sub>4</sub> (0.5 wt.%) as a catalyst, molar ratio of oil/alcohol 1:18 and a temperature of 65 °C during 5 h [43]. Then, by transesterification reaction, five oil samples converted to biodiesel. Oil/alcohol molar ratio of 1:6 and potassium hydroxide as a catalyst (1 wt.% of oil) was selected. Reaction was done at 60 °C during 4 h under total reflux condition and stirring.

### 2.2. Density measurement

The hydrometer method described in ASTM Standard D1298 was used for measuring density of pure biodiesel fuels and biodiesel-diesel blends in the ambient temperature (AT), 298.15 K, 313.15 K, 323.15 K, 333.15 K, 343.15 K and 353.15 K. Lin-Tech art. no. 600 702-4 glass hydrometers with accuracy of three decimal and a Lin-Tech art. LT/DB-55100/M density bath with ±0.01°C temperature controller were used in the measurement. The test was repeated three times for each sample and the average of results was reported.

Table 2 shows measured density of pure components (biodiesels and diesel) at different temperatures. Also biodiesel-diesel blends density with volume fractions of 0.8, 0.6, 0.4 and 0.2 are presented in Table 3. According to these tables density is increases by temperature reducing and biodiesel volume fraction increases.

**Table 2: Density and kinematic viscosity of pure biodiesels and diesel**

Temperature (K)	SOB	COB	SFOB	WOB	ETB	Diesel
	$\rho$ (g/cm <sup>3</sup> )					
293.15	0.8825	0.8805	0.8830	0.8765	0.8700	0.8265
298.15	0.8780	0.8765	0.8790	0.8720	0.8656	0.8231
313.15	0.8680	0.8660	0.8685	0.8615	0.8555	0.8125
323.15	0.8605	0.8590	0.8615	0.8545	0.8465	0.8060
333.15	0.8540	0.8520	0.8545	0.8460	0.8400	0.7995
343.15	0.8450	0.8435	0.8460	0.8390	0.8335	0.7920
353.15	0.8378	0.8365	0.8390	0.8310	0.8265	0.7865
	$\nu$ (cSt)					
313.15	4.404	4.791	4.439	4.767	5.034	2.932
323.15	3.637	3.953	3.656	3.894	4.113	2.445
333.15	3.085	3.320	3.080	3.280	3.433	2.077
343.15	2.659	2.848	2.641	2.803	2.901	1.803
353.15	2.331	2.465	2.293	2.417	2.501	1.587
363.15	2.124	2.189	2.016	2.121	2.179	1.407

### 2.3. Kinematic viscosity measurement

Measuring of kinematic viscosity for each sample from 313.15 K to 363.15 K by steps of 10 K was done according to ASTM Standard D445. Cannon-Fenske type glass capillary viscometers (size no. 75) and a Lin-Tech art. LT/VB-37000/M viscosity bath with  $\pm 0.01$  °C temperature control were used. To determine kinematic viscosity, the efflux time that is the time for a known volume of liquid flowing under gravity to pass through the viscometer tube was multiplied by the viscometer constant. Viscometer constant is obtained from calibration curve provided by manufacture at 313.15 K and 373.15 K that it was linearly interpolated to other temperatures. Such as density the test was repeated three times for each sample and the results were averaged.

Kinematic viscosity of pure component (biodiesels and diesel) and also biodiesel-diesel blends at different temperatures are shown in Tables 2 and 3, respectively. Values of these tables are shown similar trend between kinematic viscosity and density under temperature and volume fraction changes of biodiesel.

## 3. Methodology

Artificial neural network has a high ability for learning and organizing of nonlinear and complex correlation. In this study for

estimating of density and kinematic viscosity of biodiesel-diesel blends ANN has been used. A brief review on ANN that used in this work was done by Eslamloueyan and Khademi [40].

### 3.1. Analyzing and using data

In this work for density estimation, reported data in literatures [16, 17 and 20] (262 data points) and measured data in this study (181 data points) have been used. From density data 70% (311 data points) for training, 15% (66 data points) for validation and 15% (66 data points) for network testing have been selected randomly. As clearly seen from Eqs. (1), (4) and (9), mixture density is dependent to temperature, components volume fraction and pure components density. Usually density was determined at 293.15 K, so in this model density expressed as a function of temperature, components volume fraction (only volume fraction of one component is sufficient, because  $v_2 = 1 - v_1$ ) and density of pure components at 293.15 K:

$$\rho_m = f(T, v_1, \rho_1, \rho_2) \quad (16)$$

Also for estimating of kinematic viscosity, reported data of literatures [3, 16, 17 and 20] (367 data points) and measured data on this study (156 data points) have been used. From all kinematic viscosity data randomly

70% (367 data points) for training, 15% (78 data point) for validation and 15% (78 data points) for network testing have been selected. According to Eqs. (2), (3), (6), (7) and (10) to (15), it was shown clearly that

kinematic viscosity of biodiesel-diesel blends is depend on temperature, components volume fraction and kinematic viscosity of pure components.

**Table 3: Density and kinematic viscosity of biodiesel-diesel blends**

Biodiesel	Volume fraction	Temperature (K)						
		AT	298.15	313.15	323.15	333.15	343.15	353.15
		$\rho$ (g/cm <sup>3</sup> )						
SOB	0.8	0.8740 <sup>a</sup>	0.8669	0.8570	0.8500	0.8410	0.8345	0.8280
	0.6	0.8610 <sup>b</sup>	0.8570	0.8445	0.8380	0.8310	0.8245	0.8175
	0.4	0.8470 <sup>c</sup>	0.8440	0.8335	0.8270	0.8200	0.8130	0.8065
	0.2	0.8360 <sup>d</sup>	0.8340	0.8235	0.8170	0.8100	0.8035	0.7970
COB	0.8	0.8710 <sup>e</sup>	0.8659	0.8555	0.8465	0.8395	0.8330	0.8265
	0.6	0.8600 <sup>f</sup>	0.8560	0.8435	0.8370	0.8300	0.8235	0.8165
	0.4	0.8475 <sup>g</sup>	0.8440	0.8340	0.8270	0.8200	0.8135	0.8070
	0.2	0.8360 <sup>h</sup>	0.8335	0.8235	0.8165	0.8100	0.8035	0.7965
SFOB	0.8	0.8720 <sup>e</sup>	0.8671	0.8570	0.8500	0.8415	0.8345	0.8280
	0.6	0.8630 <sup>i</sup>	0.8570	0.8450	0.8380	0.8315	0.8250	0.8180
	0.4	0.8470 <sup>j</sup>	0.8445	0.8340	0.8270	0.8205	0.8135	0.8070
	0.2	0.8370 <sup>k</sup>	0.8340	0.8240	0.8170	0.8105	0.8035	0.7970
WOB	0.8	0.8690 <sup>l</sup>	0.8624	0.8520	0.8435	0.8365	0.8295	0.8230
	0.6	-	0.8535	0.8415	0.8345	0.8275	0.8210	0.8140
	0.4	0.8465 <sup>m</sup>	0.8425	0.8320	0.8255	0.8185	0.8120	0.8055
	0.2	0.8360 <sup>c</sup>	0.8330	0.8230	0.8160	0.8095	0.8025	0.7960
ETB	0.8	0.8635 <sup>l</sup>	0.8575	0.8455	0.8385	0.8320	0.8250	0.8180
	0.6	0.8535 <sup>g</sup>	0.8480	0.8380	0.8310	0.8240	0.8175	0.8105
	0.4	0.8430 <sup>n</sup>	0.8400	0.8300	0.8230	0.8165	0.8095	0.8030
	0.2	0.8345 <sup>o</sup>	0.8320	0.8220	0.8150	0.8085	0.8015	0.7950
		Temperature (K)						
			313.15	323.15	333.15	343.15	353.15	363.15
		$\nu$ (cSt)						
SOB	0.8		3.952	3.294	2.787	2.402	2.103	1.913
	0.6		3.658	3.060	2.568	2.203	1.929	1.720
	0.4		3.375	2.814	2.389	2.061	1.826	1.610
	0.2		3.085	2.566	2.227	1.911	1.701	1.519
COB	0.8		4.313	3.569	2.975	2.546	2.208	1.945
	0.6		3.839	3.199	2.691	2.389	2.002	1.761
	0.4		3.502	2.918	2.469	2.138	1.870	1.654
	0.2		3.160	2.636	2.227	1.920	1.677	1.506
SFOB	0.8		4.045	3.358	2.846	2.435	2.122	1.866
	0.6		3.641	3.004	2.548	2.215	1.910	1.687
	0.4		3.356	2.787	2.364	2.042	1.781	1.575
	0.2		3.013	2.511	2.125	1.834	1.606	1.424
WOB	0.8		4.333	3.560	2.981	2.559	2.217	1.951
	0.6		3.835	3.168	2.672	2.297	2.008	1.757
	0.4		3.473	2.884	2.434	2.118	1.840	1.612
	0.2		3.176	2.639	2.238	1.945	1.693	1.544
ETB	0.8		4.516	3.721	3.092	2.631	2.276	2.009
	0.6		4.042	3.337	2.786	2.375	2.075	1.813
	0.4		3.590	2.957	2.495	2.135	1.861	1.643
	0.2		3.187	2.643	2.233	1.925	1.686	1.477
Ambient Temperature: <sup>a</sup> 288.35 K, <sup>b</sup> 292.35 K, <sup>c</sup> 293.35 K, <sup>d</sup> 294.75 K, <sup>e</sup> 290.95 K, <sup>f</sup> 291.95 K, <sup>g</sup> 292.75 K, <sup>h</sup> 293.95 K, <sup>i</sup> 290.55 K, <sup>j</sup> 293.55 K, <sup>k</sup> 292.95 K, <sup>l</sup> 288.75 K, <sup>m</sup> 292.45 K, <sup>n</sup> 293.75 K, <sup>o</sup> 294.15 K								

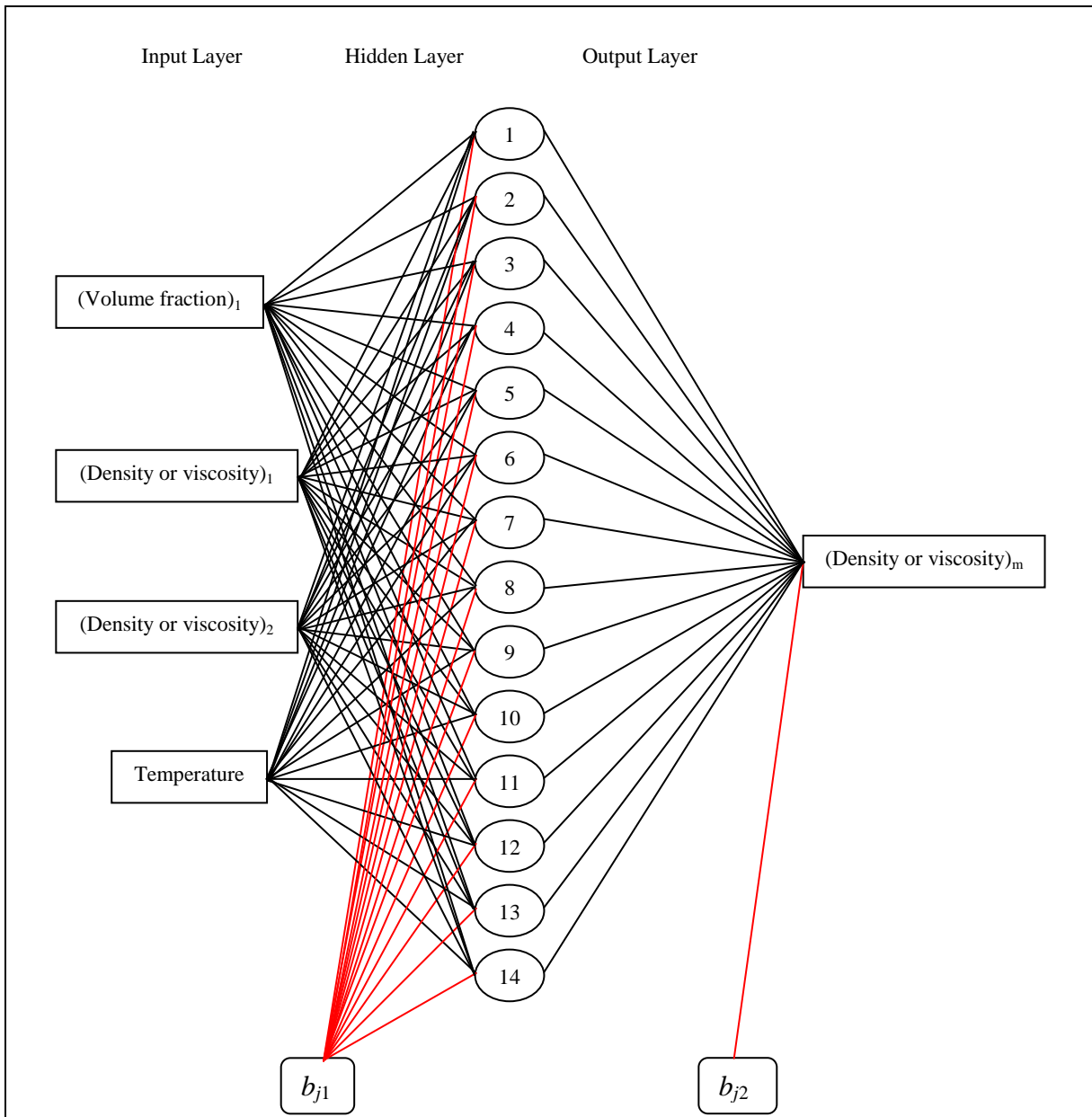


Figure1: Schematic of three-layer ANN

Table4: Statistical data for estimating density and kinematic viscosity ANN model

	$v_1$	$\rho_1\ or\ \nu_1$	$\rho_2\ or\ \nu_2$	$T\ (K)$	$\rho_m\ or\ \nu_m$
	Density ( $g/cm^3$ )				
Minimum	0.00	0.8700	0.8265	288.35	0.7779
Maximum	1.00	0.8869	0.8853	373.15	0.8869
Average	0.49	0.8793	0.8511	328.80	0.8388
Median	0.49	0.8816	0.8344	333.15	0.8371
Standard deviation	0.34	0.0063	0.0261	25.66	0.0245
	Kinematic viscosity (cSt)				
Minimum	0.00	2.872	2.650	268.15	1.140
Maximum	1.00	7.030	5.140	373.15	12.320
Average	0.49	4.652	3.159	326.32	3.606
Median	0.49	4.439	2.932	323.15	2.957
Standard deviation	0.33	1.095	0.697	28.54	2.193

Usually kinematic viscosity measured at 313.15 K, so a model for kinematic viscosity has been presented that considered as a function of temperature, components volume fraction and kinematic viscosity of pure components at 313.15 K:

$$\nu_m = f(T, \nu_1, \nu_2) \quad (17)$$

In Table 4 statistical data (minimum, maximum, average, median and standard deviation) of density and kinematic viscosity ANNs are given.

### 3.2. Neural network training

After determining of input data, designing of ANN can be started. Here a three-layer feed forward network has been used. Schematic of one three-layer ANN has been shown in Figure1. Number of neurons in hidden layer should be minimum value and if training error of network with this number of neurons be higher than desired value, number of neurons increased one by one to receive a value lower than desired value [44].

By applying neural network on density data, optimum number of neurons at hidden layer is equal to 14. Same result by applying kinematic viscosity data is obtained (hidden neurons are equal to 14). At the obtained models in hidden and output layers transfer function of 'tansig' and 'purelin' are used, respectively. These functions defined as below:

$$f_{tansig}(\chi) = \frac{\exp(\chi) - \exp(-\chi)}{\exp(\chi) + \exp(-\chi)} \quad (18)$$

$$f_{purelin}(\chi) = \chi \quad (19)$$

Also output of a neuron is calculated by follow equation:

$$O_j = f_{purelin} \left\{ \sum_{k=1}^m W_{jk}^{OL} \left[ f_{tansig} \left( \sum_{i=1}^n (W_{ji}^{HL} x_i) + b_j^{HL} \right) \right] + b_j^{OL} \right\} \quad (20)$$

For training, algorithm of Levenberg-Marquard (LM) [45-47] is used. Performance function of this algorithm is

mean relative error (MRE), maximum number of epochs is 500 and performance goal is  $10^{-5}$ .

**Table 5: Determining number of optimum hidden neurons for estimating density and kinematic viscosity**

No. of neurons	Mean relative error			
	Train	Test	Validation	Total
	Density			
9	0.035	0.041	0.030	0.035
10	0.024	0.041	0.030	0.028
11	0.026	0.045	0.033	0.030
12	0.024	0.043	0.031	0.028
13	0.033	0.045	0.034	0.035
14	0.018	0.034	0.025	<b>0.021</b>
15	0.024	0.047	0.031	0.028
16	0.025	0.039	0.026	0.027
17	0.024	0.043	0.035	0.028
18	0.024	0.043	0.034	0.028
19	0.023	0.043	0.034	0.027
20	0.026	0.041	0.029	0.029
	Kinematic viscosity			
9	2.47	2.67	2.66	2.53
10	1.07	0.92	1.15	1.06
11	0.91	0.81	1.02	0.91
12	1.08	1.09	1.29	1.11
13	1.41	1.16	1.41	1.37
14	0.65	0.91	0.92	<b>0.73</b>
15	0.93	0.85	1.05	0.94
16	0.71	0.84	0.91	0.76
17	0.80	1.14	0.93	0.87
18	0.89	1.04	1.08	0.94
19	0.69	0.76	0.93	0.74
20	0.70	0.88	0.81	0.74

## 4. Results and discussion

Table5 is shown values of mean relative error by applying of density and kinematic viscosity data, respectively. As clearly shown for 14 neurons in hidden layer MRE of density model for training, validation, testing and sum of data are 0.018, 0.034, 0.025 and 0.021%, respectively and for kinematic viscosity these data are 0.65,

0.91, 0.92 and 0.73%, respectively. Parameters (weights and biases) of three-layer networks for optimum hidden neurons (14 neurons) are presented in Table 6.

The obtained results from best model for density (a model with 14 neurons in hidden layer) are presented in Figure 2. This figure is for training, validation and testing data, respectively. In this figure obtained data from model versus experimental data was plot. Also relative errors of these data in this figure are shown. As shown in this figure maximum relative error for training, validation and testing data are 0.128, -0.126 and -0.340%, respectively. Similar results for kinematic viscosity were presented in Figure3. Maximum relative error of kinematic viscosity for training, validation and testing data are -5.26, 4.48 and 4.49%,

respectively. According to figures 2 and 3, high accuracy of neural network models clearly was shown.

At the end, the obtained results from presented model for density and viscosity are compared with previous literatures correlations. Table 7 is shown MRE of different systems by using of ANN model and Eq. (9). Procedure of calculating constant of Eq. (9) and determining of MRE were presented in the literature [20]. As shown in Table 7, total mean relative error using ANN model is 0.021%, whilst this value by Eq. (9) is 0.05%. This result indicated high accuracy of ANN model.

Also in Table 8, the obtained results from MRE of ANN kinematic viscosity model by Eqs. (10)-(15) are shown.

**Table6: ANN parameters for density and kinematic viscosity model**

Hidden layer				Output layer		
Weights			Biases	Weights		Bias
$v_i$	Pure property of component 1	Pure property of component 2	$T$		Mixture property	
Density						
0.4719	-0.1732	2.9137	0.2090	-4.2529	1.1029	-0.1515
-10.1182	-2.5341	18.7466	11.0542	28.4736	-0.0167	
0.7864	1.0067	-0.5699	0.2475	-2.0678	-0.0938	
7.4009	9.5311	-7.9452	0.6754	-10.0158	-0.0071	
-0.0957	-0.3513	-0.1610	0.0684	0.1743	-8.6405	
0.5124	1.8628	-3.8499	-0.2978	-0.6998	2.8627	
-0.3567	-1.9457	-4.5235	0.0964	1.5938	7.3664	
0.5915	1.5449	-3.6007	-0.2877	-0.8591	-3.4727	
-0.3183	2.8638	7.8001	-0.1030	-3.7612	4.4869	
-0.0902	-0.6276	0.7522	-0.0141	-0.1154	4.0639	
0.3400	0.6787	-0.1888	-0.1155	1.7572	7.9830	
0.0437	0.9981	1.7827	-0.0358	1.1778	-2.0352	
-5.5192	-2.0237	3.5873	3.2664	-2.0021	-0.0045	
-0.1781	-0.2058	0.3803	0.0387	-0.9525	5.0045	
Viscosity						
0.6716	0.7793	-2.9788	0.3544	-2.8699	0.0456	1.8057
0.3336	-0.6476	0.2026	-0.7999	-1.7326	-3.2503	
-1.4954	5.5684	-2.7373	-1.8453	5.5961	0.1043	
-0.1762	-1.5085	-2.9985	-0.4724	0.4611	-0.6058	
0.0979	-0.4111	-0.0527	-1.6214	-0.2926	-0.2732	
-1.1118	-0.8162	-0.2109	3.9466	3.6056	-0.3018	
-0.0896	-2.4146	-0.3017	-7.2350	-4.3923	-0.0450	
-0.2118	0.0888	-0.1868	0.8762	0.9414	-3.6443	
2.2076	0.0429	-4.3310	-1.5786	2.6240	0.0535	
-0.6445	-3.0423	-1.3719	0.7583	3.1307	-0.8372	
0.0868	-0.6330	0.7422	-0.0911	3.2023	1.5906	
0.3336	0.8078	-0.1286	0.6666	2.0568	-1.4431	
-0.8266	-1.8260	-4.3292	0.7107	-0.5798	0.4321	
0.1986	-1.3305	-2.8712	9.6392	8.4631	-1.7426	

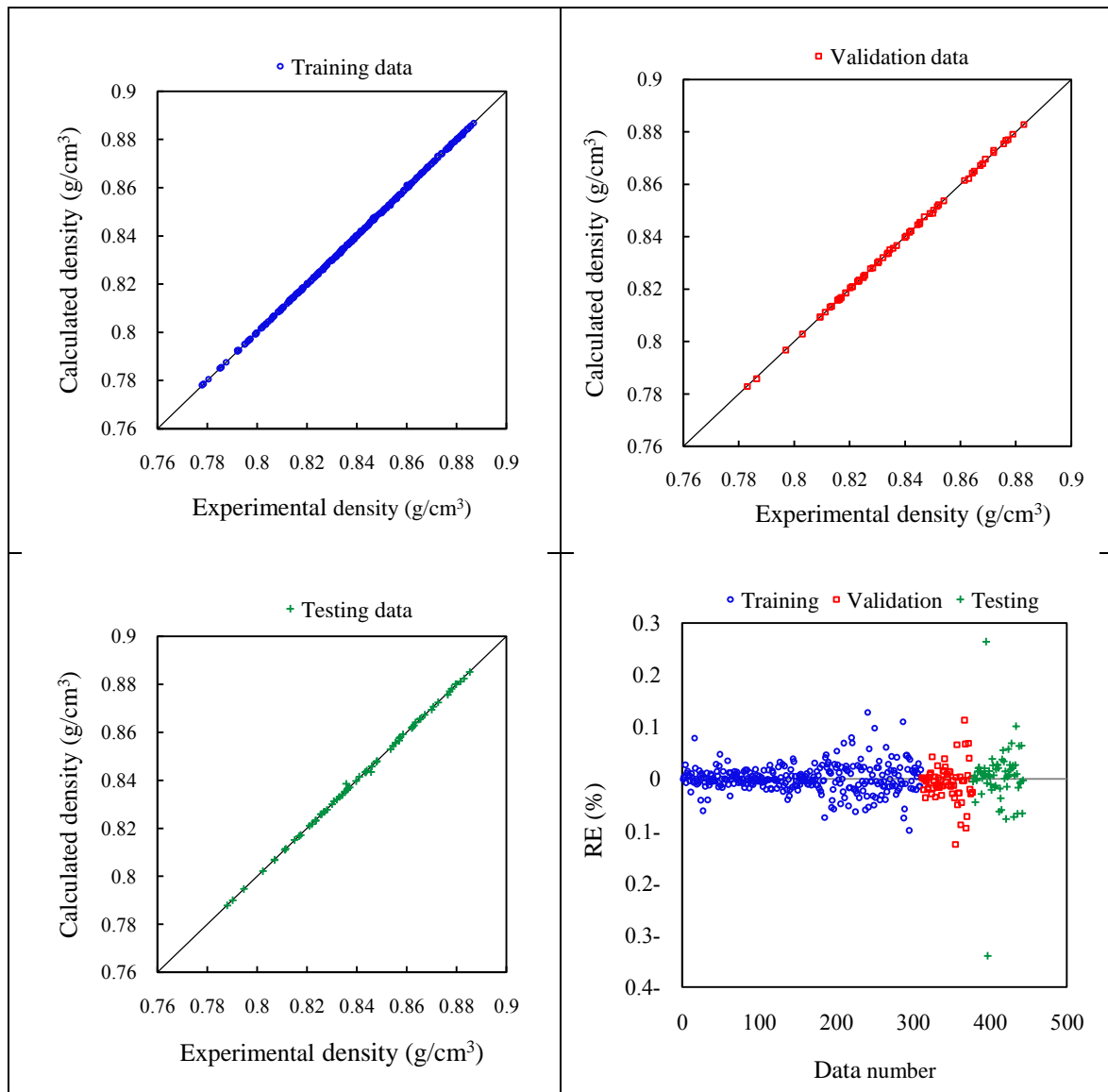
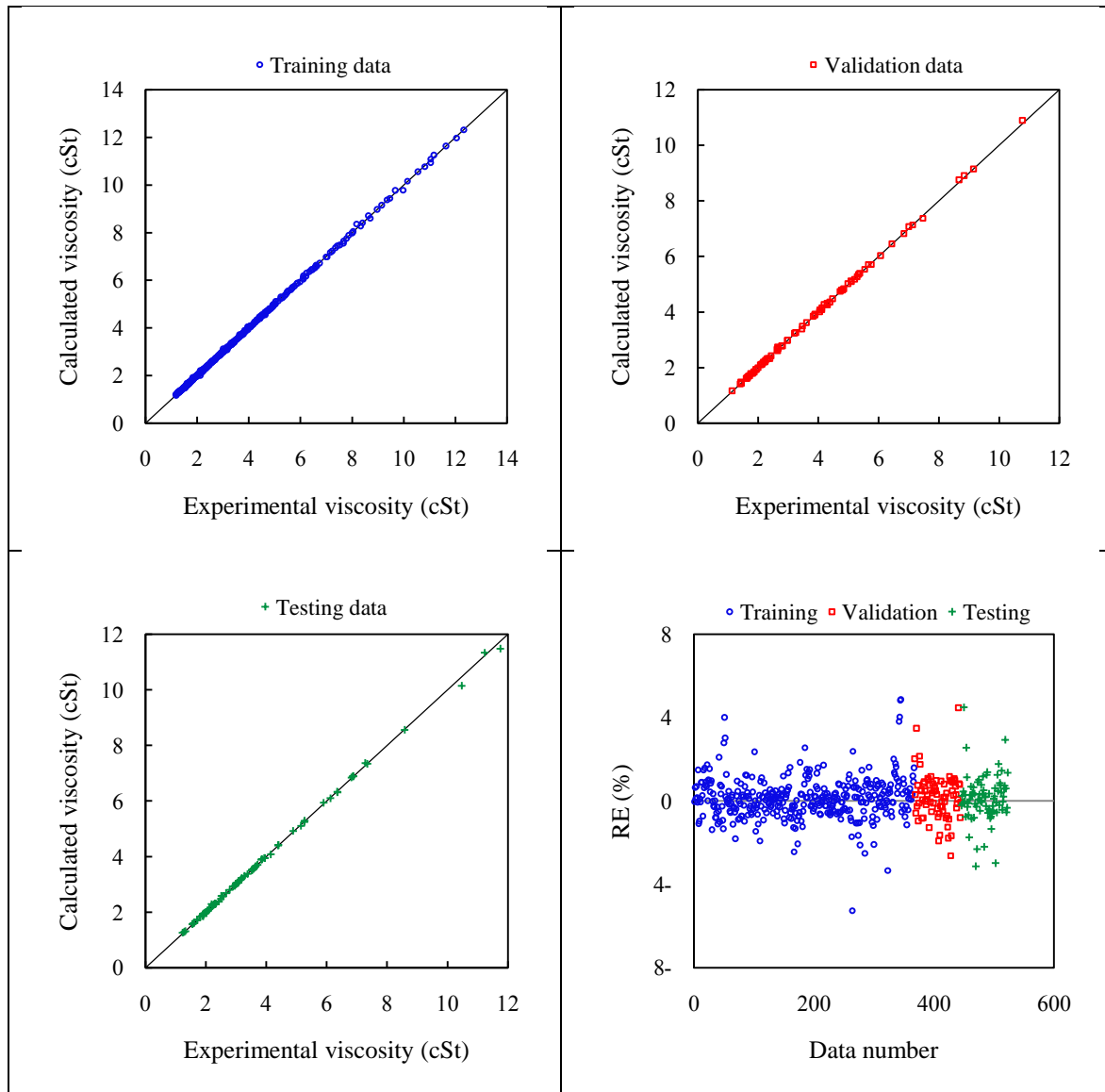


Figure2: Obtained results from ANN density model (training, validation and testing data)

Table7: Comparing results of ANN and Eq. (9)

System	NDP	MRE	
		ANN	Eq. (9)
Biodiesel (1) + ULSD (2) [20]	72	0.013	0.020
Colza biodiesel (1) + Coconut biodiesel (2) [17]	55	0.011	0.040
Soybean biodiesel (1) + Coconut biodiesel (2) [17]	45	0.024	0.060
Cotton seed biodiesel (1) + Babassu biodiesel (2) [16]	45	0.016	0.040
Soybean biodiesel (1) + Babassu biodiesel (2) [16]	45	0.013	0.050
Pure biodiesels and diesel (this work)	42	0.035	0.094
SOB (1) + Diesel (2) (this work)	28	0.032	0.075
COB (1) + Diesel (2) (this work)	28	0.028	0.072
SFOB (1) + Diesel (2) (this work)	28	0.041	0.076
WOB (1) + Diesel (2) (this work)	27	0.023	0.065
ETB (1) + Diesel (2) (this work)	28	0.023	0.061
Total	443	0.021	0.050





**Figure3: Obtained results from ANN kinematic viscosity model (training, validation and testing data)**

**Table8: Comparing results of ANN and Eqs. (10)-(15)**

System	NDP	MRE						
		AN N	Eq. (10)	Eq. (11)	Eq. (12)	Eq. (13)	Eq. (14)	Eq. (15)
Biodiesel (1) + ULSD (2) [20]	72	0.93	4.79	2.10	2.39	2.13	2.17	3.43
Commercial Biodiesel (1) + Low sulfur petrodiesel (2) [3]	105	0.62	2.77	1.74	1.76	1.81	1.74	1.73
Colza biodiesel (1) + Coconut biodiesel (2) [17]	55	0.4	5.50	2.17	2.27	2.22	2.27	2.54
Soybean biodiesel (1) + Coconut biodiesel (2) [17]	45	0.96	5.36	2.13	2.18	2.23	2.17	2.34
Cotton seed biodiesel (1) + Babassu biodiesel (2) [16]	45	0.46	5.50	2.24	2.26	2.30	2.28	2.28
Soybean biodiesel (1) + Babassu biodiesel (2) [16]	45	0.47	6.36	2.62	2.68	2.58	2.69	2.77
Pure biodiesels and diesel (this work)	36	0.82	2.08	1.09	1.10	1.34	1.12	1.22
SOB (1) + Diesel (2) (this work)	24	1.01	2.29	1.34	1.29	1.30	1.36	1.41
COB (1) + Diesel (2) (this work)	24	0.90	1.85	0.99	1.00	1.01	1.00	1.15
SFOB (1) + Diesel (2) (this work)	24	1.66	1.83	0.87	0.89	1.06	0.87	0.97
WOB (1) + Diesel (2) (this work)	24	0.57	1.97	0.94	1.01	1.03	0.96	1.28
ETB (1) + Diesel (2) (this work)	24	0.58	2.02	0.89	0.95	1.04	0.93	1.22
Total	523	0.73	3.88	1.77	1.85	1.84	1.81	2.08

In this study, the procedure for calculation of parameters in Eqs. (10)-(15) is similar to the literature [20]. In Table 8 MRE of each system using of ANN model and Eq. (10)-(15) are presented. Total mean relative error of ANN kinematic viscosity model and Eqs. (10)-(15) are 0.73, 3.88, 1.77, 1.85, 1.84, 1.81 and 2.08%, respectively. Therefore artificial neural network model has shown a higher accuracy than presented correlation in the previous literatures.

## 5. Conclusion

In this study for estimating density and kinematic viscosity of biodiesel-diesel blends, artificial neural network (three-layer feed forward neural network with LM algorithm, 'tansig' transfer function in hidden layer and 'purelin' transfer function in output layer) have been used.

The published literature data for density and kinematic viscosity of biodiesel-diesel blends and this work data (SOB, COB, SFOB, WOB and ETB) have been used for learning of network. 70% of data (311 data points for density and 367 data points for kinematic viscosity) for training, 15% of data (66 data points for density and 78 data points for kinematic viscosity) for validation and 15% of data (66 data points for density and 78 data points for kinematic viscosity) for testing were selected.

By applying networks on density and kinematic viscosity data, number of optimum neurons in hidden layer for each two models (density and kinematic viscosity) is 14. For these numbers of neuron mean relative error of density on training, validation and testing data were obtained 0.018, 0.034 and 0.025%, respectively. Also mean relative error for kinematic viscosity on training, validation and testing data were obtained 0.65, 0.91 and 0.92%, respectively.

Finally total mean relative errors for data of density was 0.021% and for kinematic viscosity was obtained 0.73% that is lower than the other correlations.

## Nomenclature

$a$	constant in Eqs. (1), (5) and (8)
$A$	constant in Eqs. (2) and (3)
$b$	constant in Eqs. (1), (5) and (8)
$B$	constant in Eqs. (2) and (3)
$b_j$	bias of $j$ th neuron
$c$	constant in Eq. (8)
$C$	constant in Eqs. (2) and (3)
$f$	transfer function, function
$O_j$	output of $j$ th neuron
$T$	temperature, K
$v$	volume fraction
$V$	volume percent, %
$w_{ji}$	synaptic weight corresponding to $i$ th synapse $j$ th neuron
$w_{jk}$	synaptic weight corresponding to $k$ th synapse $j$ th neuron
$x_i$	$i$ th input signal to th neuron
<i>Greek letter</i>	
$\alpha$	constant in Eq. (9)
$\beta$	constant in Eq. (9)
$\chi$	input value of neural network
$\delta$	constant in Eq. (9)
$\phi$	constant in Eqs. (10) to (15)
$\gamma$	constant in Eqs. (10) to (15)
$\lambda$	constant in Eqs. (10) to (15)
$\rho$	density, g/cm <sup>3</sup>
$\nu$	kinematic viscosity, cSt
$\omega$	constant in Eqs. (10) to (15)
<i>Subscripts</i>	
1	component 1
2	component 2
$m$	Mixture
<i>Superscripts</i>	
$HL$	hidden layer
$OL$	output layer

## References:

- 1- Geacai, S., Iulian, O. and Nita, I. (2015) "Measurement, correlation and prediction of biodiesel blends viscosity." *Fuel*, Vol. 143, pp.268–274.

- 2- Gülüm, M. and Bilgin, A. (2015). "Density, flash point and heating value variations of corn oil biodiesel–diesel fuel blends." *Fuel Processing Technology*, Vol.134, pp.456–464.
- 3- Knothe, G., Gerpen, J.V. and Krahl, J. (2005). *The biodiesel handbook*. IL: AOCS Press.
- 4- Ma, F.R. and Hanna, M.A. (1999). "Biodiesel production: a review." *Bioresour. Technol.*, Vol. 70, pp. 1–15.
- 5- Benjumea, P., Agudelo, J. and Agudelo, A. (2008). "Basic properties of palm oil biodiesel–diesel blends." *Fuel*, Vol. 87, pp. 2069–2075.
- 6- Yoon, S.H., Park, S.H. and Lee, C.S. (2008). "Experimental investigation on the fuel properties of biodiesel and its blends at various temperatures." *Energy Fuels*, Vol. 22, pp. 652–656.
- 7- Alptekin, E. and Canakci, M. (2008). "Determination of the density and the viscosities of biodiesel–diesel fuel blends." *Renewable Energy*, Vol. 33, pp. 2623–2630.
- 8- Tesfa, B., Mishra, R., Gua, F. and Powles, N. (2010) "Prediction models for density and viscosity of biodiesel and their effects on fuel supply system in CI engines." *Renewable Energy*, Vol. 35, pp. 2752-2760.
- 9- Shu, Q., Yang, B., Yang, J. and Qing, S. (2007) "Predicting the viscosity of biodiesel fuels based on the mixture topological index method." *Fuel*, Vol. 86, pp. 1849–1854.
- 10- Barabás, I. (2015). "Liquid densities and excess molar volumes of ethanol+biodiesel binary system between the temperatures 273.15 K and 333.15 K." *Journal of Molecular Liquids*, Vol. 204, pp. 95–99.
- 11- Freitas, S.V.D., Pratas, M.J., Ceriani, R., Lima, A.S. and Coutinho, J.A.P. (2011). "Evaluation of predictive models for the viscosity of biodiesel." *Energy Fuels*, Vol. 25, pp. 352–358.
- 12- Ceriani, R., Gonçálves, C.B., Rabelo, J., Caruso, M., Cunha, A.C.C., Cavaleri, F.W. et al. (2007). "Group contribution model for predicting viscosity of fatty compounds." *J. Chem. Eng. Data*, Vol. 52, pp. 965-972.
- 13- Krisnangkura, K., Yimsuwan, T. and Pairintra, R. (2006). "An empirical approach in predicting biodiesel viscosity at various temperatures." *Fuel*, Vol. 85, pp. 107–113.
- 14- Pratas, M.J., Freitas, S., Oliveira, M.B., Monteiro, S.C., Lima, A.S. and Coutinho, J.A.P. (2010). "Densities and viscosities of fatty acid methyl and ethyl esters." *J. Chem. Eng. Data*, Vol. 55, pp. 3983–3990.
- 15- Pratas, M.J., Freitas, S., Oliveira, M.B., Monteiro, S.C., Lima, A.S. and Coutinho, J.A.P. (2011). "Densities and viscosities of minority fatty acid methyl and ethyl esters present in biodiesel." *J. Chem. Eng. Data*, Vol. 56, pp. 2175–2180.
- 16- Nogueira, C.A., Feitosa, F.X., Fernandes, F.A.N., Santiago, R.S. and de Sant'Ana, H.B. (2010). "Densities and viscosities of binary mixtures of babassu biodiesel + cotton seed or soybean biodiesel at different temperatures." *J. Chem. Eng. Data*, Vol. 55, pp. 5305–5310.
- 17- Feitosa, F.X., Rodrigues, M.L., Veloso, C.B., Cavalcante, C.L., Albuquerque, M.C.G. and de Sant'Ana, H.B. (2010). "Viscosities and densities of binary mixtures of coconut + colza and coconut + soybean biodiesel at various temperatures." *J. Chem. Eng. Data*, Vol. 55, pp. 3909–3914.
- 18- Tate, R.E., Watts, K.C., Allen, C.A.W. and Wilkie, K.I. (2006). "The densities of three biodiesel fuels at temperatures up to 300 °C." *Fuel*, Vol. 85, pp. 1004–1009.
- 19- Nita, I., Geacai, S. and Iulian, O. (2011). "Measurements and correlations of physico-chemical properties to composition of pseudo-binary mixtures with biodiesel." *Renewable Energy*, Vol. 36, pp. 3417-3423.
- 20- Ramírez-Verduzco, L.F., García-Flore, B.E., Rodríguez-Rodríguez, J.E. and Jaramillo-Jacob, A.R. (2011). "Prediction of the density and viscosity in biodiesel blends at various temperatures." *Fuel*, Vol. 90, pp. 1751–1761.

- 21- Tate, R.E., Watts, K.C., Allen, C.A.W. and Wilkie, K.I. (2006). "The viscosities of three biodiesel fuels at temperatures up to 300 °C." *Fuel*, Vol. 85, pp. 1010–1015.
- 22- Tat, M.E. and Van Gerpen, J.H. (1999). "The kinematic viscosity of biodiesel and its blends with diesel fuel." *J. Am. Oil Chem. Soc.*, Vol. 76, pp. 1511-1513.
- 23- Yuan, W., Hansena, A.C., Zhang, Q. and Tan, Z. (2005). "Temperature-dependent kinematic viscosity of selected biodiesel fuels and blends with diesel fuel." *J. Am. Oil Chem. Soc.*, Vol. 82, pp. 195-199.
- 24- Krisnangkura, K., Sansa-ard, C., Aryusuk, K., Lilitchan, S. and Kittiratanapiboon, K. (2010). "An empirical approach for predicting kinematic viscosities of biodiesel blends." *Fuel*, Vol. 89, pp. 2775–2780.
- 25- Grunberg, L. and Nissan, A.H. (1949). "Mixture law for viscosity." *Nature*, Vol. 164, pp. 799–800.
- 26- Joshi, R.M. and Pegg, M.J. (2007). "Flow properties of biodiesel fuel blends at low temperatures." *Fuel*, Vol. 86, pp. 143–151.
- 27- Bhat, N. and McAvoy, T.J. (2000). "Use of neural nets for dynamic modeling and control of chemical process systems." *Comput. Chem. Eng.*, Vol. 14, pp. 573-583.
- 28- Moradi, M.R., Nazari, K., Alavi, S. and Mohadesi, M. (2013). "Prediction of Equilibrium Conditions for Hydrate Formation in Binary Gaseous Systems Using Artificial Neural Networks." *Energy Technol.*, Vol. 1, pp. 171-176.
- 29- Moradi, G., Mohadesi, M. and Moradi, M.R. (2013). "Prediction of wax disappearance temperature using artificial neural networks." *J. Pet. Sci. Eng.*, Vol. 108, pp. 74-81.
- 30- Mohadesi, M., Moradi, G. and Mousavi, H.-S. (2014). "Estimation of Binary Infinite Dilute Diffusion Coefficient Using Artificial Neural Network." *J. Chem. Pet. Eng.*, Vol. 48, pp. 27-45.
- 31- Molga, E. and Cherbanski, R. (1999). "Hybrid first-principle-neural network approach to modeling of the liquid-liquid reacting system." *Chem. Eng. Sci.*, Vol. 54, pp. 2467-2473.
- 32- Fissore, D., Barresi, A.A. and Manca, D. (2004). "Modeling of methanol synthesis in a network of forced unsteady-state ring reactors by artificial neural networks for control purposes." *Chem. Eng. Sci.*, Vol. 59, pp. 4033-4041.
- 33- Kito, S., Satsuma, A., Ishikura, T., Niwa, M., Murakami, Y. and Hattori, T. (2004). "Application of neural network to estimation of catalyst deactivation in methanol conversion." *Catal. Today*, Vol. 97, pp. 41-47.
- 34- Papadokonstantakis, S., Machefer, S., Schnitzleni, K. and Lygeros, A.I. (2005). "Variable selection and data pre-processing in NN modeling of complex chemical processes." *Comput. Chem. Eng.*, Vol.29, pp. 1647-1659.
- 35- Omata, K., Nukai, N. and Yamada, M. (2005). "Artificial neural network aided design of a stable Co-MgO catalyst of high-pressure dry reforming of methane." *Ind. Eng. Chem. Res.*, Vol. 44, pp. 296-301.
- 36- Himmelblau, D. (2008). "Accounts of experiences in the application of artificial neural networks in chemical engineering." *Ind. Eng. Chem. Res.*, Vol. 47, pp. 5782-5796.
- 37- Hashemipour, H., Baroutian, S., Jamshidi, E. and Abazari, A. (2009). "Experimental study and artificial neural networks simulation of activated carbon synthesis in fluidized bed reactor." *Int. J. Chem. Reactor Eng.*, Vol. 7, A80.
- 38- Nabavi, R., Salari, D., Niaei, A. and Vakil-Baghmisheh, M.-T. (2009). "A neural network approach for prediction of main product yields in methanol to olefins process." *Int. J. Chem. Reactor Eng.*, Vol. 7, A26.

- 39- Khataee, A and Khani, A. (2009). "Modeling of nitrate adsorption on granular activated carbon (GAC) using artificial neural network (ANN)." *Int. J. Chem. Reactor Eng.*, Vol. 7, A5.
- 40- Eslamloueyan, R. and Khademi, M.H. (2009). "Estimation of thermal conductivity of pure gases by using artificial neural networks." *Int. J. Thermal. Sci.*, Vol. 48, pp. 1094–1101.
- 41- Eslamloueyan, R. and Khademi, M.H. (2009). "Using artificial neural networks for estimation of thermal conductivity of binary gaseous mixtures." *J. Chem. Eng. Data*, Vol. 54, pp. 922–932.
- 42- Eslamloueyan, R. and Khademi, M.H. (2010). "A neural network-based method for estimation of binary gas diffusivity." *Chemom. Intell. Lab. Syst.*, Vol. 104, pp. 195–204.
- 43- Encinar, J.M., Sánchez, N., Martínez, G. and García, L. (2011). "Study of biodiesel production from animal fats with high free fatty acid content." *Bioresour. Technol.*, Vol. 102, pp. 10907–10914.
- 44- Haykin, S. (1999). *Neural networks: a comprehensive foundation*. 2<sup>nd</sup> Ed. Englewood Cliffs, NJ: Prentice-Hall.
- 45- Levenberg, K. (1944). "A method for the solution of certain problems in least squares." *SIAM J. Numer. Anal.*, Vol. 16, 588–604.
- 46- Marquardt, D. (1963). "An algorithm for least-squares estimation of nonlinear parameters." *SIAM J. Appl. Math.*, Vol. 11, pp. 431–441.
- 47- Hagan, M.T. and Menhaj, M. (1994). "Training feedforward networks with the Marquardt algorithm." *IEEE Trans. Neural. Netw.*, Vol. 5, pp. 989–993.